Taylor & Francis
Taylor & Francis Group

RESEARCH PAPER

Importin α5 negatively regulates importin β1-mediated nuclear import of Newcastle disease virus matrix protein and viral replication and pathogenicity in chicken fibroblasts

Zhiqiang Duan[a,b], Haixu Xu[c], Xinqin Ji[a,b], Jiafu Zhao[a,b], Houqiang Xu[a,b], Yan Hu[b], Shanshan Deng[b], Shunlin Hu[c], and Xiufan Liu[c]

[a]Key Laboratory of Animal Genetics, Breeding and Reproduction in The Plateau Mountainous Region, Ministry of Education, Guizhou University, Guiyang, China; [b]College of Animal Science, Guizhou University, Guiyang, China; [c]Key Laboratory of Animal Infectious Diseases of Ministry of Agriculture, Yangzhou University, Yangzhou, China

ABSTRACT

The matrix (M) protein of Newcastle disease virus (NDV) is demonstrated to localize in the nucleus via intrinsic nuclear localization signal (NLS), but cellular proteins involved in the nuclear import of NDV M protein and the role of M's nuclear localization in the replication and pathogenicity of NDV remain unclear. In this study, importin β1 was screened to interact with NDV M protein by yeast two-hybrid screening. This interaction was subsequently confirmed by co-immunoprecipitation and pull-down assays. *In vitro* binding studies indicated that the NLS region of M protein and the amino acids 336–433 of importin β1 that belonged to the RanGTP binding region were important for binding. Importantly, a recombinant virus with M/NLS mutation resulted in a pathotype change of NDV and attenuated viral replication and pathogenicity in chicken fibroblasts and SPF chickens. In agreement with the binding data, nuclear import of NDV M protein in digitonin-permeabilized HeLa cells required both importin β1 and RanGTP. Interestingly, importin α5 was verified to interact with M protein through binding importin β1. However, importin β1 or importin α5 depletion by siRNA resulted in different results, which showed the obviously cytoplasmic or nuclear accumulation of M protein and the remarkably decreased or increased replication ability and pathogenicity of NDV in chicken fibroblasts, respectively. Our findings therefore demonstrate for the first time the nuclear import mechanism of NDV M protein and the negative regulation role of importin α5 in importin β1-mediated nuclear import of M protein and the replication and pathogenicity of a paramyxovirus.

Introduction

Newcastle disease virus (NDV), a member of the genus *Avulavirus* in the family *Paramyxoviridae*, is an important avian pathogen that causes substantial economic losses to the poultry industry worldwide [1,2]. The genome of NDV is a non-segmented, single-stranded, negative-sense RNA encoding at least six proteins in the order 3'-NP-P-M-F-HN-L-5' [3]. Of all these viral structural proteins, the matrix (M) protein has the least molecular weight of around 40 kDa and forms an outer protein shell around the nucleocapsid, which constitutes the bridge between the viral envelope and the nucleocapsid [4]. Like most paramyxovirus M proteins, the NDV M protein is a multifunctional nucleocytoplasmic shuttling protein and plays crucial roles in NDV life cycle [5]. In addition to functioning for the assembly and budding of progeny virions in the cytoplasm and at

the cell membrane later in infection [6], the NDV M protein is localized in the nucleus and nucleolus early in infection and remains in the nucleoli throughout infection [7–9]. The nuclear-nucleolar localization of NDV M protein is thought to inhibit host cell transcription and protein synthesis similar to the human respiratory syncytial virus (HRSV) [10] and vesicular stomatitis virus (VSV) M protein [11], and also ensure that viral replication and transcription in the cytoplasm proceed smoothly, which is by analogy with the measles virus (MeV) M protein [12]. Numerous studies have demonstrated that the nuclear and nucleolar localization of viral proteins depend on their own nuclear localization signal (NLS) and nucleolar localization signal (NoLS) as well as the cellular transport proteins [13–15]. Our recent study found that the nucleolar protein B23 targets NDV M protein to the nucleoli by interacting with the amino

acids 30–60 (a putative NoLS) of M protein and enhances viral replication ability [16]. Previous study has shown that NDV M protein enters the nucleus via a bipartite NLS (KKGKKVIFDKIEEKIRR) independent of other viral proteins [17], but cellular proteins involved in the nuclear import of NDV M protein and the biological functions of this nuclear localization still remain unknown.

It has been demonstrated that nuclear transport of proteins carrying NLS through the nuclear envelope-embedded nuclear pore complexes (NPCs) is mediated by members of the importin superfamily including importin α and importin β [18–20]. The classical paradigm for nuclear import pathway is that importin α directly recognizes and binds to the NLS of cargo proteins, and then importin $\beta1$ directs binding of the binary complex to the cytoplasmic side of the NPC. The translocation of GDP-bound small GTPase Ran (RanGDP) conjunct ternary complex through the NPC is mediated by NTF2 via interaction with nucleoporins. Once inside the nucleus, binding of GTP-bound small GTPase Ran (RanGTP) to importin $\beta1$ causes the dissociation of the ternary complex [21,22]. Thus, cargo proteins are transported into the nucleus. In general, classical NLSs including monopartite and bipartite NLSs are imported by importin $\alpha/\beta1$ heterodimer, while non-classical NLSs can be more complex in length, sequence and amino acid composition that are imported by importin $\beta1$ [21]. However, recent studies have found that classical NLSs can also be recognized and binded by importin $\beta1$ or homologs without the participation of importin α [23–25]. Moreover, some studies even confirmed that importin α can act as negative regulators for the nuclear import of some cargo proteins mediated by importin $\beta1$ alone [26,27]. Therefore, such diverse nuclear import pathways are receiving increasingly attention.

Many recent studies have proven that nuclear localization of viral proteins is crucial for viral replication and propagation [28–31]. For example, nuclear localization of the nucleocapsid protein of porcine respiratory and reproductive syndrome virus is essential for optimal virus replication and inhibition of cellular antiviral processes [32], and the successful production of infectious virions and efficient propagation of Japanese encephalitis virus require the nuclear localization of core protein [33,34]. For the members of paramyxoviruses, the M proteins of HRSV, Sendai virus (SeV), Nipah virus (NiV), and NDV all have the molecular mass less than 40 kDa and localize in the nucleus during the course of virus infection [5]. Although functional NLSs in the M proteins of these viruses have been characterized, so far, only the HRSV M protein is demonstrated to be recruited into the nucleus through direct recognition by

importin $\beta1$ [35]. In addition, nuclear localization of M protein is important for the generation of HRSV progeny virions and is associated with the pathogenesis of viral infection [36]. Therefore, we speculated that the cellular importin members might also participate in the nuclear import of NDV M protein and regulate the replication and pathogenicity of NDV.

In this study, importin $\beta1$ was identified to be the nuclear transport receptor of NDV M protein and mediate the nuclear import of NDV M protein by binding its NLS region via the RanGTP-dependent pathway. Further studies showed that NLS mutation in the M protein disrupted its nuclear localization and reduced viral replication in chicken fibroblasts and attenuated viral replication and pathogenicity in SPF chickens. Interestingly, importin $\alpha5$ was demonstrated to be a negative regulator in importin $\beta1$-mediated nuclear import of M protein and the replication and pathogenicity of NDV, as importin $\alpha5$ deletion remarkably increased the nuclear accumulation of M protein and the replication ability and pathogenicity of NDV in chicken fibroblasts. Our studies will provide deep insights into understanding the more functions of M's nuclear localization in the life cycle and pathogenesis of NDV.

Results

Yeast two-hybrid screening of NDV M-interacting cellular proteins

To define cellular proteins that interact with NDV M protein, a yeast two-hybrid screening strategy was employed. The NDV M protein was used as the bait for screening the cDNA library generated from DF-1 cells. The results showed that six colonies (No. 3 to 8) could grow on the auxotrophic medium SD/-Ade/-His/-Trp/-Leu and turn blue in the presence of X-α-gal, which had the same presentation as the positive control transformed with pGBKT7-53 and pGADT7-T (No. 2) (Fig. 1A and B). However, the negative control could neither not grow nor turn blue on the medium SD/-Ade/-His/-Trp/-Leu/X-α-gal (No. 1). To further confirm the true interaction with M protein in yeast, β-galactosidase colony-lift filter assay was performed. We found that yeast colonies co-transformed with the pGADT7-derivative plasmids and pGBKT7-M plasmid all turned blue within 30 min, which was similar to the positive control (Fig. 1C). The nucleotide sequences of six colonies from the cDNA library were then sequenced and analyzed. The results showed that the sequences of six clones had the right open reading frame (ORF) in frame with the AD coding region, and five cellular proteins containing the interaction region were identified by bioinformatics
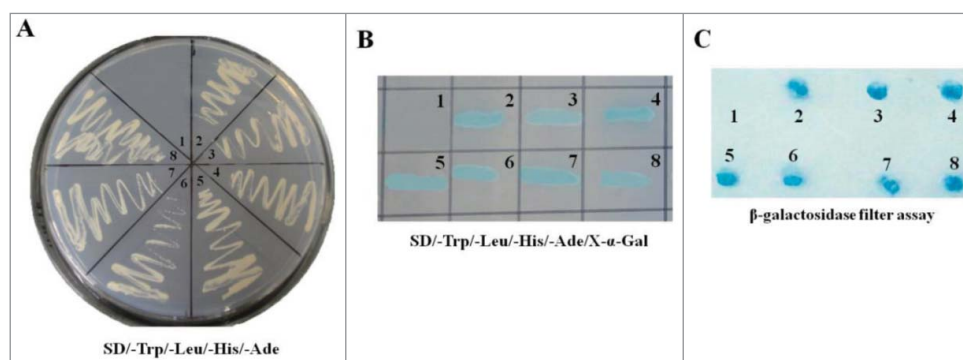
Figure 1. Screening the cellular proteins interacting with NDV M protein through yeast two-hybrid assay. (A) The bait plasmid pGBKT7-M transformed AH109 was mated with yeast Y187 containing pGADT7-Rec with the cDNA library of DF-1 cells. The suspected positive colonies were screened on the auxotrophic medium SD/-Trp/-Leu/-His/-Ade. N0.1 was the negative control and no.2 was the positive control. (B) The yeast colonies obtained from (A) were cultured on the SD/-Trp/-Leu/-His/-Ade/X-α-gal medium. The colonies growing on this medium and turning blue are the indication of interaction of the two expressed proteins. (C) The yeast colonies obtained from (A) were transferred into nitrocellulose filters and assayed for β-galactosidase activity to verify the interaction between NDV M protein and the cellular proteins.

analysis (Table 1). Fortunately, of all these proteins, importin β1 is demonstrated to be a karyopherin that transports multiple proteins owing NLS into the nucleus [23]. Therefore, we conclude that NDV M protein may bind importin β1 to enter the nucleus.

NDV M protein interacts with importin β1 in vivo and in vitro

To verify the interaction between NDV M protein and importin β1, we first performed co-immunoprecipitation assay with DF-1 cells transiently transfected with plasmid encoding Myc-importin β1 and infected with NDV. Expression of the fusion protein Myc-importin β1 and viral M protein was confirmed with anti-Myc and anti-M antibodies, respectively (Fig. 2A, upper panel). In addition, the M protein and importin β1 in cell supernatants could be immunoprecipitated with each other when using anti-Myc or anti-M antibody (Fig. 2A, middle and lower panels). Next, in vitro binding assay of the fusion protein GST-M to the purified His-importin β1 protein showed that His-importin β1 was pulled-down by GST-M protein but not by GST (Fig .2B). These results suggest that that NDV M protein physically interacts with importin β1 protein in vivo and in vitro.

Previous studies have shown that importin β1 mediates the nuclear import of cargo proteins by binding their

NLS [23–25]. Here, the binding studies revealed that the NLS region in the M protein was important for importin β1 binding, since GST-M protein with the mutated NLS lost its binding activity to importin β1 (Fig. 2C). In addition, His-importin β1 deleting residues 336 to 433 ($\triangle$336-433) could not be pulled down by GST-M (Fig. 2D), indicating that the amino acids 336–433 of importin β1 was essential for interaction with M. It is reported that human importin β1 contains importin-β N-terminal (IBN_N) domain at the N-terminus and several "HEAT repeat" motifs that mostly occupy the C-terminal portion [37]. After comparison with the amino acids of human importin β1, the residues 336 to 433 in chicken belonged to the 8–10 HEAT repeats, which were also the RanGTP binding region. Thus, we demonstrate that the NLS region of NDV M protein and the 8–10 HEAT repeats of importin β1 are important for interaction with each other.

NLS mutation in the M protein attenuates the replication and pathogenicity of NDV

Now that the NLS of M protein was essential for its interaction with importin β1, we investigated the effect of M/NLS mutation on the virulence, replication ability and pathogenicity of NDV. The results of virus rescue showed that hemagglutination (HA)-positive allantoic

Table 1. Comparison between positive clones and similar sequences in GenBank.

Homologous genes (mRNA)	Number of similar clone	GenBank Accession No.	Homologous region	Homology* (%)
Eukaryotic translation elongation factor 2	1 (clone 3)	NM_205368.1	1783-2307 (CDS: 31–2607)	100
Serine and arginine rich splicing factor 3	1 (clone 4)	NM_001195554.1	136-510 (CDS: 115–609)	99
Matrin 3	2 (clone 5 and 8)	NM_204147.1	2017-2460 (CDS: 328–3036)	100
Importin β1	1 (clone 6)	XM_015299473.1	1007-1300 (CDS: 181–2811)	99
Bromodomain containing 2	1 (clone 7)	NM_001030674.1	1717-2016 (CDS: 1–2190)	100

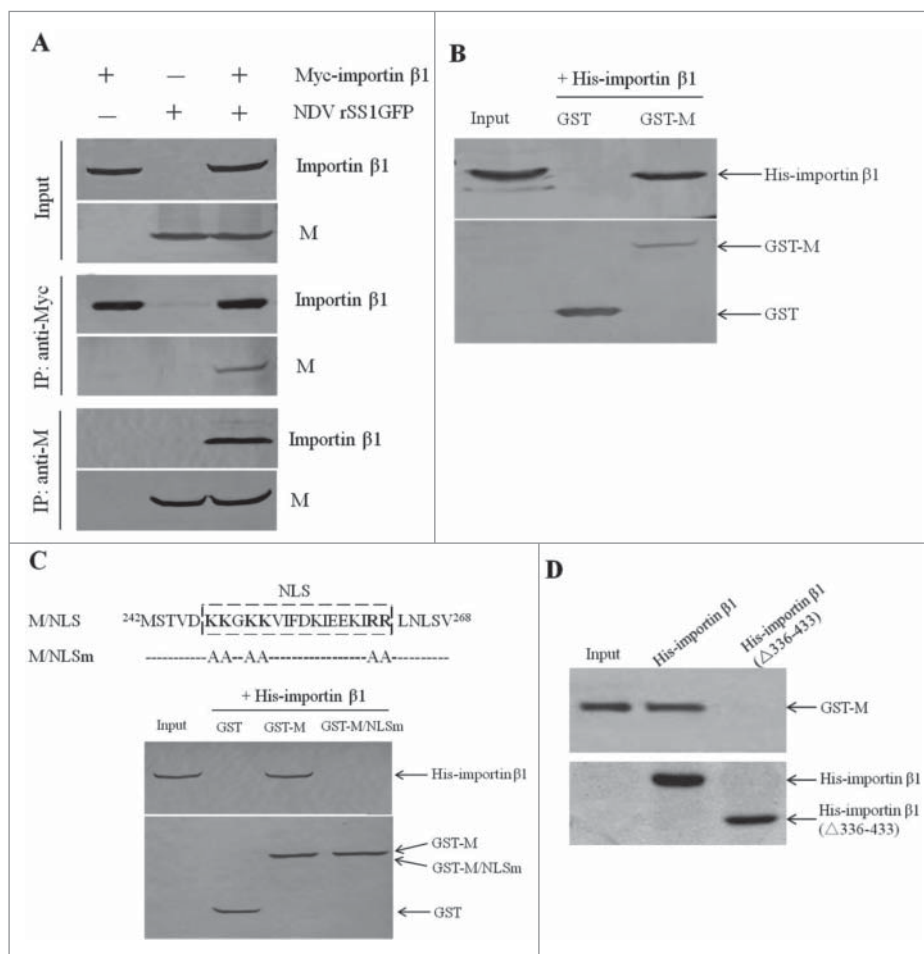*Homology comparison with Gallus sequences.

Figure 2. NDV M protein interacts with importin $\beta1$ *in vivo* and *in vitro*. (A) Reciprocal co-immunoprecipitation assay of Myc-importin $\beta1$ and NDV M protein in DF-1 cells. DF-1 cells transfected with plasmid expressing Myc-importin $\beta1$ were infected with NDV at an MOI of 0.1. Cells were lysed at 24 h post-infection, and co-immunoprecipitation assay was performed using either anti-Myc (middle panel) or anti-M (lower panel) antibodies. Immunoprecipitated proteins were detected by Western blotting using anti-M or anti-Myc antibodies. (B) The interaction between M and importin $\beta1$ was verified by GST pull-down assay. GST or GST-M or His-importin $\beta1$ protein was expressed in *E. coli* BL21 (DE3) and purified on Glutathione-Sepharose beads or His*Bind resins, respectively. The purified GST or GST-M protein (3 μg) was immobilized on Gluthatione-Sepharose beads and then incubated with the purified His-importin $\beta1$ (3 μg) for 2 h at 4°C. The beads were washed with transport buffer and the bound proteins were eluted from the beads and detected by Western blotting. (C and D) GST-M/NLSm or His-importin $\beta1(\triangle336\text{-}433)$ was expressed in *E. coli* BL21 (DE3) and then purified as described above. GST pull-down and His pull-down assays were performed to identify the interaction domains between M and importin $\beta1$.

fluid was directly detected in the parental virus rSS1GFP, but three extra egg passages were required for the M/NLS mutant virus rSS1GFP-M/NLSm to be detected by HA test, indicating that the growth of the mutant virus in chicken eggs was slowed down. To determine the stability of M gene mutant virus, the rescued virus rSS1GFP-M/NLSm was plaque purified and passaged five times in 10-day-old specific pathogen free (SPF) chicken eggs. Sequence analysis of the whole-genome of the mutant virus after five passages showed that the introduced M/NLS mutation was unaltered (see Figure S1 in the supplemental material), and no additional mutations were observed in the M gene and other viral genes (data not shown). The immunofluorescence results showed that NLS mutation absolutely disrupted the

nuclear localization of M protein in virus-infected cells (Fig. 3A). Meanwhile, the biological characteristics detection revealed that M/NLS mutation significantly extended the MDT of rSS1GFP-M/NLSm (>120 h) in embryonated chicken eggs compared to rSS1GFP (54 ± 2 h), and the ICPI value of rSS1GFP-M/NLSm (1.67 ± 0.01) was lower than that of rSS1GFP (1.88 ± 0.02) (Table 2), indicating that M/NLS mutation could result in a pathotype change of NDV. In addition, the plaques produced by the viruses indicated that cells infected with rSS1GFP developed large and more plaques with a mean size of 2.85 ± 0.35 mm, while cells infected with rSS1GFP-M/NLSm developed much less and smaller plaques with a mean size of 0.87 ± 0.30 mm (Fig. 3B). On the other hand, multicycle growth kinetics experiments
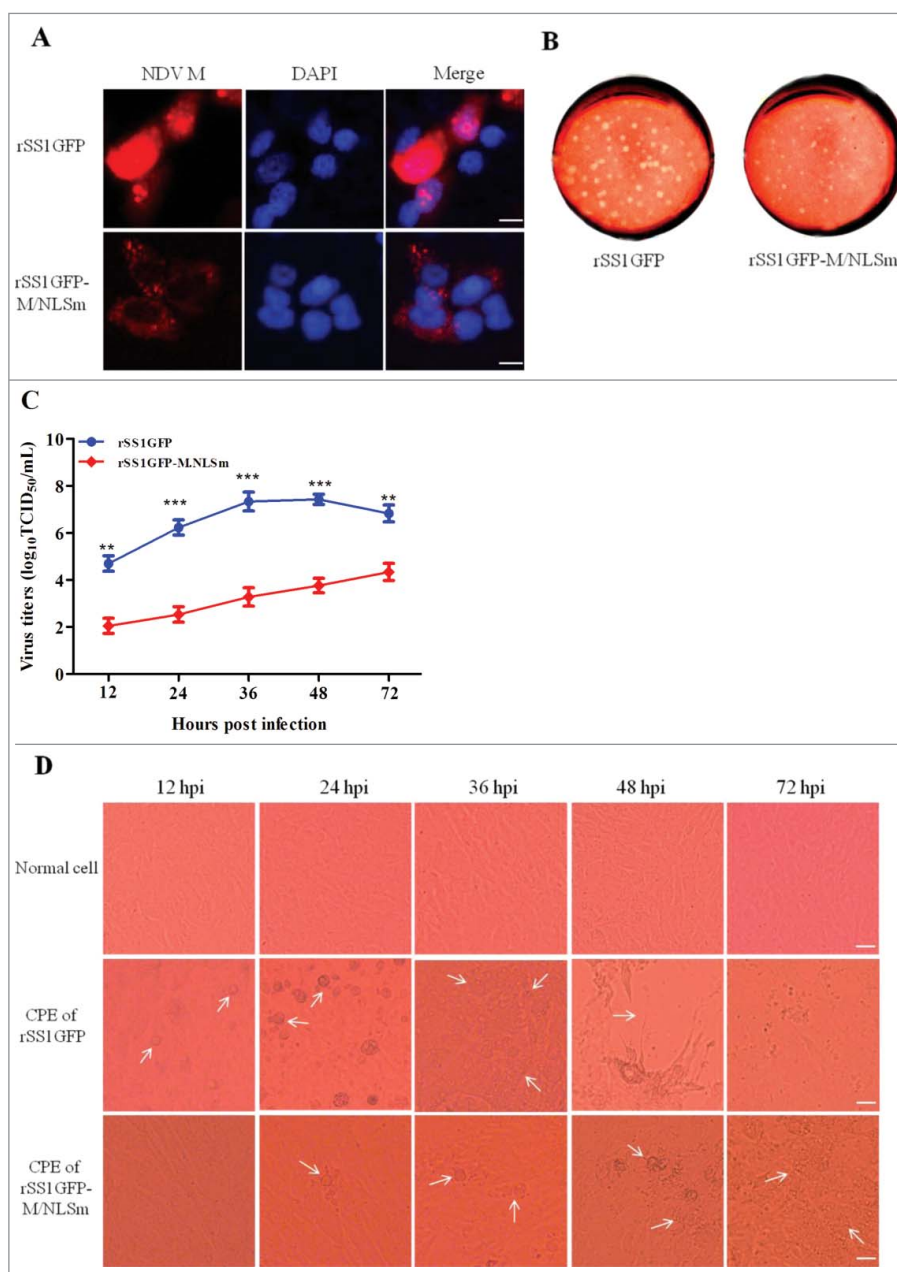
Figure 3. M/NLS mutation reduces the replication ability of NDV in cells. (A) The immunofluorescence assay was used to examine the subcellular localization of NDV M protein in rSS1GFP and rSS1GFP-M/NLSm infected DF-1 cells at 12 hpi. DAPI was used to stain nuclei. Original magnification was 1×200. (B) The shape and size of plaques formed by rSS1GFP and rSS1GFP-M/NLSm in DF-1 cells. DF-1 cells in six-well plates were infected with serial tenfold dilutions of the virus for 1 h. After adsorption, the inoculum was removed and replaced with the medium containing 2% FBS and 1% agar. The overlay medium supplemented with 0.1% neutral red was added after 36 h incubation. Plaques were observed after a further 48 h of incubation. (C) Virus titers were determined in DF-1 cells at the indicated time points. Each data point on the curve indicates the mean $\pm$ SD of three independent experiments. P values < 0.001 are represent with[***] and p values <0.01 are represent with [**]. (D) The CPE was observed in virus-infected DF-1 cells at the indicated time points. The images were obtained using the phase-contrast microscope. Original magnification was 1×200.

Table 2. Biological characteristics of the parental and mutant viruses[*].

Virus	Pathogenicity		Virus titer		
	MDT (h)	ICPI	EID_{50}/ml	$TCID_{50}$/ml	HA
rSS1GFP	54 ± 2	1.88 ± 0.02	10⁸].67]	10⁸].79]	8 log₂
rSS1GFP-M/NLSm	>120	1.67 ± 0.01	10⁵].34]	10⁶].17]	4 log₂

[*]MDT, mean death time; ICPI, intracerebral pathogenicity index; EID_{50}, 50% egg infectious dose; $TCID_{50}$, 50% tissue culture infective dose.

revealed that the virus titers of rSS1GFP-M/NLSm were remarkably reduced in comparison to that of rSS1GFP from 12 to 72 hpi ($P<0.01$) (Fig. 3C). Meanwhile, the cytopathic effect (CPE) in rSS1GFP infected cells started at 12 hpi and cell monolayer was absolutely destroyed at 72 hpi, but the CPE in rSS1GFP-M/NLSm infected cells started at 24 hpi and cell monolayer was still existent at 72 hpi (Fig. 3D), which showed much slighter and slower CPE than that of rSS1GFP-infected cells at the same time points.

The *in vivo* pathogenesis assessment of M/NLS mutant virus rSS1GFP-M/NLSm in 4-week-old SPF chickens was then evaluated. The resulting survival curves were shown in Fig. 4A. Birds inoculated with the parental virus rSS1GFP exhibited slight depression at 3 days post-infection (dpi), severe depression (3/ 10), wing drop (2/10), hemiparesis/paralysis (3/10), and death (2/10) at 4 dpi, and 100% mortality by 5 dpi. At necropsy, all euthanized chickens presented severe gross lesions in multiple organs, such as conjunctivitis, hemorrhage of the throat, trachea, thymus, duodenum mucosa, and proventriculus, multifocal necrosis of the spleen, and marked atrophy of thymus and bursa of Fabricius at 4–5 dpi. In comparison, birds inoculated with the mutant virus rSS1GFP-M/ NLSm presented delayed and slight depression (4/10) at 5 dpi, severe depression (2/10) and one death (1/ 10) at 6 dpi, and two death (2/10) at 7 dpi, but there were no death in the subsequent days. Virus titration assays showed that the mutant virus rSS1GFP-M/ NLSm had little replication ability in spleen, thymus and bursa of Fabricius at 5 dpi; by contrast, the
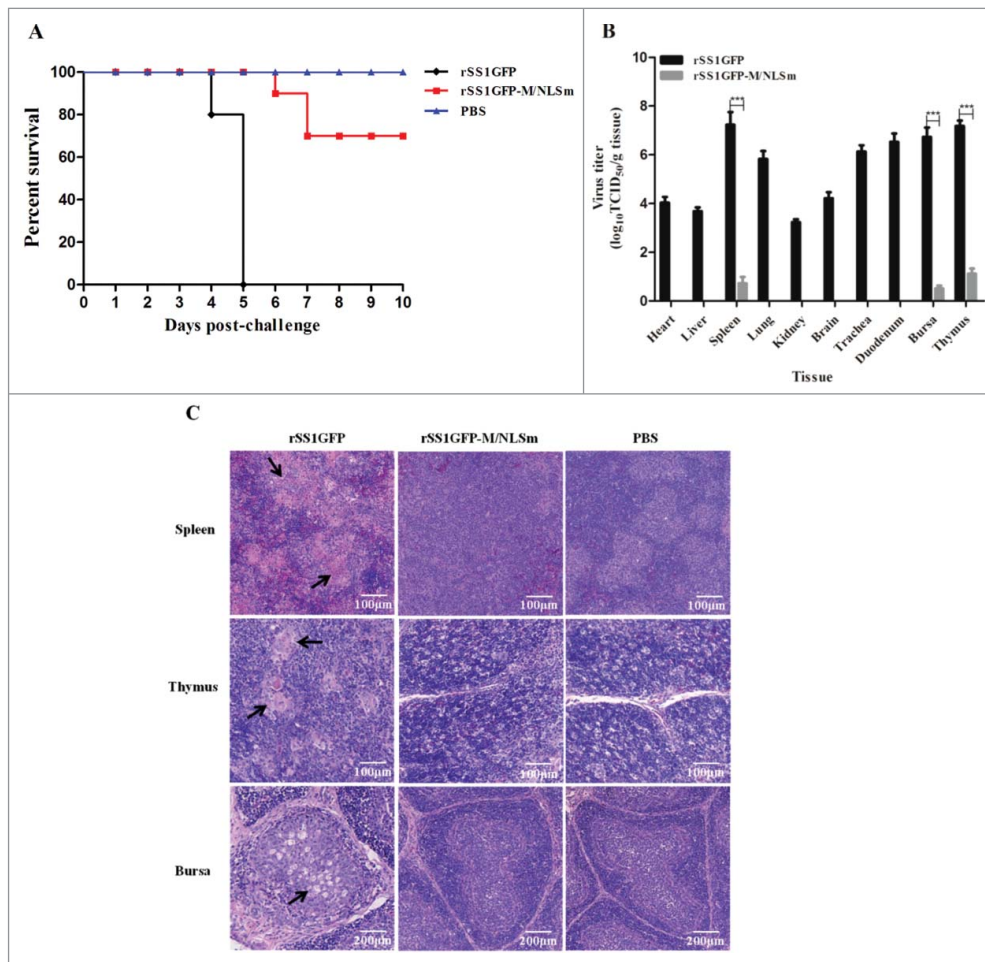

Figure 4. M/NLS mutation attenuates the replication and pathogenicity of NDV in chickens. (A) Survival curves of 4-week-old SPF chickens (n = 10 for each group). Birds were inoculated with rSS1GFP or rSS1GFP-M/NLSm at a dose of $10^{5.0}$ EID$_{50}$/100 μL per bird, or with 100 μL PBS as the negative control. The birds were monitored for clinical signs daily for 10 dpi. (B) Viral load in the collected tissues of 4-week-old chickens (n = 3) infected with the two viruses at 5 dpi. Viral titers were determined in DF-1 cells and presented as $\log_{10}$TCID$_{50}$ g^{-1} tissue. Asterisks indicate a statistically significant difference between the titers of the two viruses. P values < 0.001 are represent with***. (C) Histopathology of lymphoid tissue samples collected from rSS1GFP or rSS1GFP-M/NLSm or PBS-inoculated 4-week-old chickens. Birds were sacrificed at 5 dpi, and the tissues were fixed with 10% neutral formalin, sectioned, and stained with hematoxylin-eosin.

parental virus rSS1GFP replicated in multiple tissues and had relatively higher virus titers in the lymphoid tissues (spleen, thymus and bursa of Fabricius) (Fig. 4B). In addition, the results of histopathology observation of the lymphoid tissues showed that birds inoculated with rSS1GFP displayed multifocal confluent coagulative necrosis, severe lymphocyte depletion, and infiltration of macrophages, whereas no apparent histopathological changes were observed in the lymphoid organs of the rSS1GFP-M/NLSm group and the control group (Fig. 4C). Taken together, these results clearly demonstrate that M/NLS mutation can not only reduce viral replication ability in chicken fibroblasts but also attenuate viral replication and pathogenicity in SPF chickens.

Nuclear import of NDV M protein requires importin β1 and RanGTP

Numerous studies have shown that importin β1 together with RanGDP and/or RanGTP participate in the nuclear import of many cargo proteins [38–42]. To identify the cellular karyopherins responsible for M nuclear targeting and further verify the nuclear import pathway of NDV M protein, two dominant-negative (DN) mutants of importin α5 (DN-importin α5) [43] and importin β1 (DN-importin β1) [44], which lack the ability to bind importin β and Ran, respectively, and nuclear import inhibitors M9M [45] or Bimax2[46] that are specific for the transportin-1 pathway or the importin α1, α3, α6 and α7 pathways, respectively, RanGTP mutant (Ran/Q69L) [47], which is deficient in GTP hydrolysis, and NTF2 mutant (NTF2/E42K) [48,49], which fails to transport RanGDP into nucleus, were first introduced to determine whether they are required for the nuclear import of NDV M protein. As shown in Fig. 5A, DF-1 cells co-transfected with plasmid pEGFP-M and plasmids encoding DsRed-DN-importin α5 or DsRed-M9M or DsRed-Bimax2 or DsRed-NTF2/E42K did not impair the nuclear localization of EGFP-M, while co-expression of either DsRed-DN-importin β1 or DsRed-Ran/Q69L inhibited the nuclear accumulation of EGFP-M. In addition, detection of the intracellular localization of EGFP-M by Western blotting also verified that the EGFP-M had the same distribution as the fluorescence microscopy (Fig. 5B).

In vitro nuclear import assay was then performed to further confirm that importin β1 and RanGTP are sufficient for the nuclear import pathway of NDV M protein. The results showed that the fusion protein GST-M-GFP was efficiently imported into the nucleus of digitonin-permeabilized HeLa cells in the presence of exogenous cytosol (Fig. 5C). However, GST-M-GFP showed no nuclear translocation with RanGTP or RanGDP alone, which is similar to the results observed in the absence of cytosol, whereas combination of purified importin β1 plus RanGTP exhibited a much stronger level of nuclear accumulation than that seen when the cytosol was added (Fig. 5C). Importantly, importin β1 plus RanGDP or importin β1 alone or replacement of RanGTP with RanQ69LGTP (importin β1 plus RanQ69LGTP) led to a small amount of nuclear accumulation of GST-M-GFP (Fig. 5C). Therefore, these results confirm that importin β1 together with RanGTP but not RanGDP are the components required to mediate the active nuclear import of NDV M protein, and this process depends on GTP hydrolysis by Ran.

Nuclear import of NDV M protein does not require importin α

Ivermectin is reported to be specific for importin α/β1-mediated nuclear import of cargoes, and has no effect on any of the other nuclear import pathways including that mediated by importin β1 alone [50]. Therefore, ivermectin was used to further verify whether NDV M protein can be imported into the nucleus without the participation of importin α. We found that there was no obvious difference in the subcellular localization of NDV M protein in rSS1GFP-infected DF-1 cells treated with ivermectin or DMSO when compared to the untreated cells at 12 hpi (Fig. 6A and B). In addition, the ivermectin- or DMSO-treated DF-1 cells also had the same characteristics in the generation of CPE and the expression of GFP when infected with rSS1GFP (Fig. 6C and D). Moreover, the replication capacity of rSS1GFP was not affected in either ivermectin or DMSO treated cells at 12 hpi and 24 hpi (Fig. 6E). These results demonstrate that nuclear import of M protein and the replication of NDV are not inhibited by ivermectin, and therefore do not require importin α.

Importin α5 interacts with NDV M protein by binding importin β1

Because some of the importin α members can act as negative regulators for importin β1-mediated nuclear import of cargo proteins, so we wanted to search for the potential importin α that may indirectly bind NDV M protein and study its role in the nuclear import process of NDV M protein. Up to now, there are seven importin α members including importin α1, α3, α4, α5, α6, α7 and α8 have been identified in
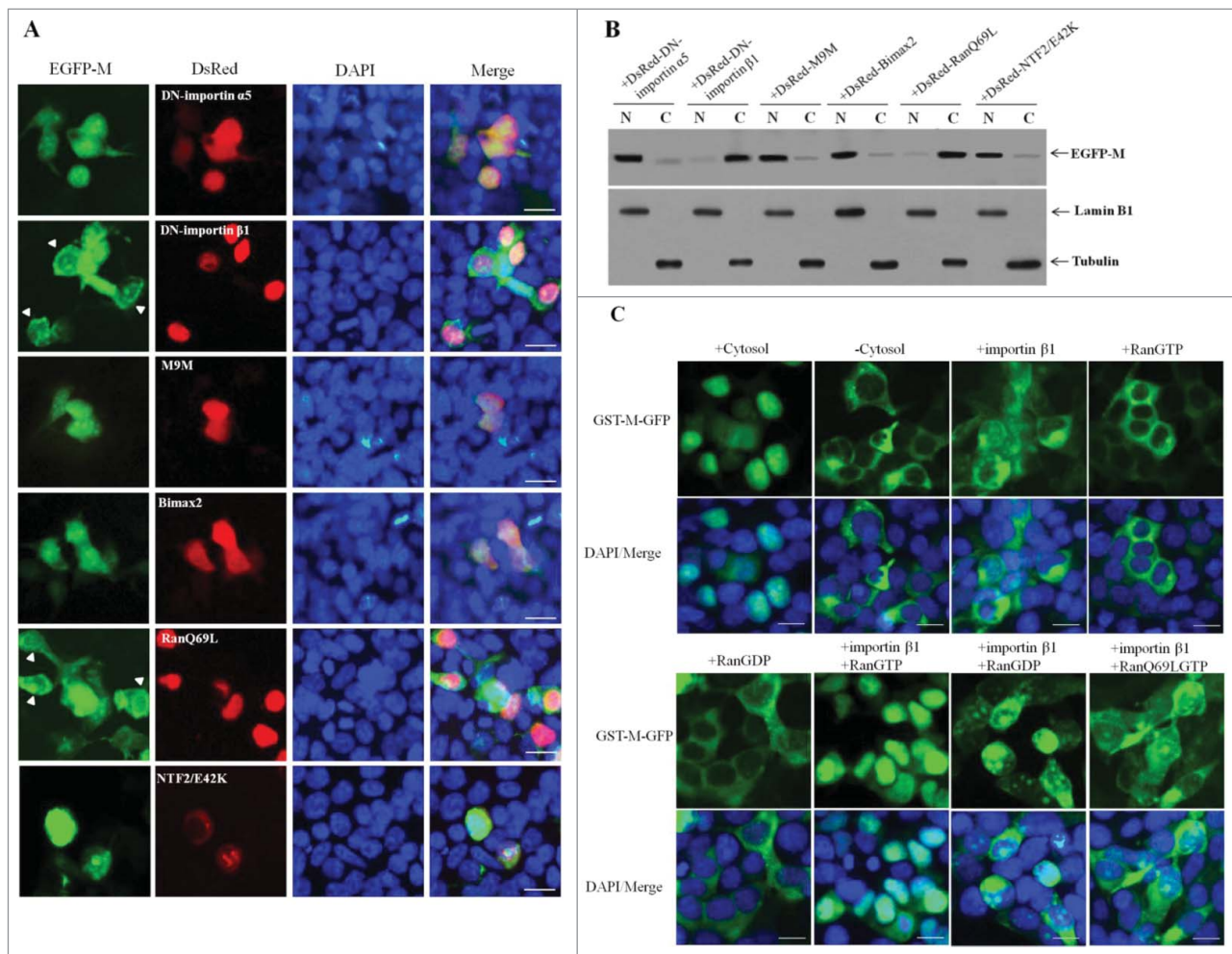
Figure 5. Nuclear import of NDV M protein requires importin β1 and RanGTP. (A) DF-1 cells were transiently co-transfected with the plasmid pEGFP-M and plasmids encoding DsRed-DN-importin α5, DsRed-DN-importin β1, DsRed-M9M, DsRed-Bimax2, DsRed-RanQ69L or DsRed-NTF2/E42K, respectively. The subcellular localization of the fusion proteins was observed under fluorescence microscope at 24 h post-transfection. DAPI was used to stain nuclei. Original magnification was 1 × 200. (B) The intracellular distribution of the fusion protein EGFP-M obtained from (A) was detected by Western blotting. Lamin B1 for the nucleus and tubulin for the cytoplasm were used as cellular markers. N represents the nucleus and C represents the cytoplasm. (C) Digitonin-permeabilized HeLa cells were incubated with GST-M-GFP in the presence of cytosol, importin β1, RanGTP, RanGDP, importin β1 plus RanGTP, importin β1 plus RanGDP, or importin β1 plus RanQ69LGTP. DAPI was used to stain nuclei. The GST-M-GFP protein was observed under fluorescence microscope. Original magnification was 1 × 200.

humans and many animals [51–53]. The immunofluorescence assay was first performed to examine the subcellular localization of these fusion proteins expressed by the recombinant eukaryotic expression vectors. As shown in Fig. 7A, besides the cytoplasmic and nuclear envelope localization of Myc-importin α1 and Myc-importin β1, the other fusion proteins including Myc-importin α3 to Myc-importin α8 and HA-M exhibited the similar localization in the nucleus. Next, the co-immunoprecipitation and pull-down assays were used to identify the potential importin α proteins that interact with NDV M protein. The results showed that both Myc-importin α5 and Myc-importin β1 could be immunoprecipitated by HA-M (Fig. 7B). However, the pull-down assay

indicated that GST-importin β1 but not GST-M could be pulled-down by His-importin α5 (Fig. 7C). Because endogenous importin α5 can interact with importin β1 in the process of transporting cargo proteins into the nucleus [21, 22], we investigated if NDV M protein can directly bind importin α5. The results of subsequent protein-binding assays showed that when GST-M immobilized on Glutathione-Sepharose beads was incubated with His-importin α5 or His-importin β1, His-importin β1 but not His-importin α5 was pulled-down by GST-M (Fig. 7D, lanes 2 and 3). However, when immobilized GST-M was incubated simultaneously with His-importin α5 and His-importin β1, both His-importin α5 and His-importin β1 were pulled-down by GST-M and
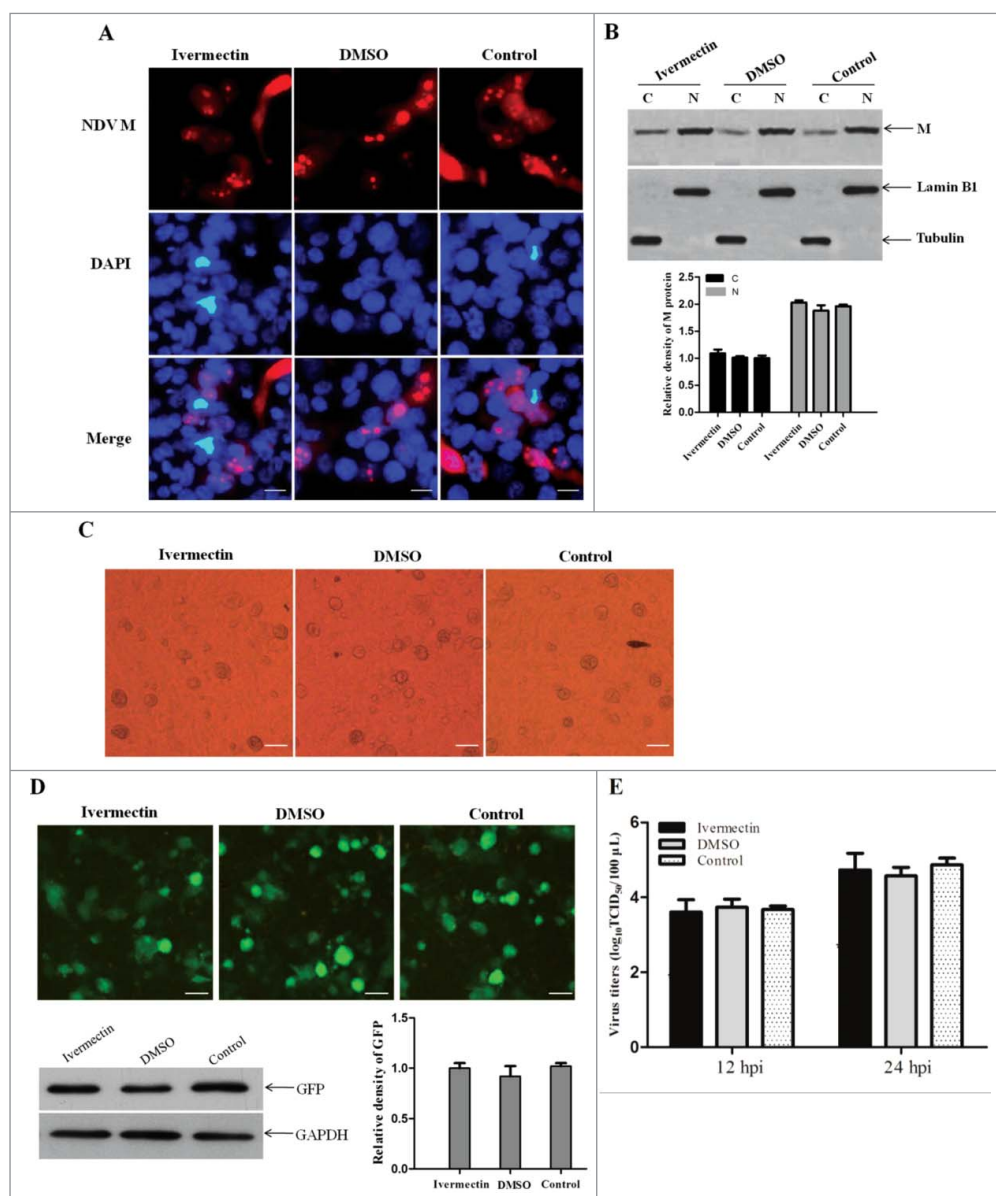
Figure 6. The nuclear import of M protein and the replication of NDV are not inhibited by ivermectin. (A) The subcellular localization of NDV M protein in virus-infected DF-1 cells treated with ivermectin or DMSO at 12 hpi. DAPI was used to stain nuclei. Original magnification was 1 × 200. (B) The intracellular distribution of NDV M protein obtained from (A) was detected by Western blotting. Lamin B1 for the nucleus and tubulin for the cytoplasm were used as cellular markers. N represents the nucleus and C represents the cytoplasm. (C) The CPE in virus-infected DF-1 cells treated with ivermectin or DMSO at 12 hpi was observed under phase-contrast microscope. Original magnification was 1 × 200. (D) The expression of GFP in virus-infected DF-1 cells was observed under fluorescence microscope and detected by Western blotting. (E) DF-1 cells were treated with the drug ivermectin or DMSO and then infected with rSS1GFP at an MOI of 0.1. The cell culture supernatants were collected at 12 and 24 hpi, and the virus titers were determined as $TCID_{50}$ in DF-1 cells.

detected by SDS-PAGE (Fig. 7D, lane 4). Therefore, these results demonstrate that importin α5 interacts with NDV M protein by binding importin β1.

Importin α5 reduces importin β1-mediated nuclear import of NDV M protein

According to the above results and for the reason that importin α5 can act as negative regulator in importin

β1-mediated nuclear import pathway, we hypothesized that importin α5 might play the inhibition function in the subcellular localization of NDV M protein. To test this hypothesis, the localization of M protein in importin β1- or importin α5-depleted DF-1 cells was investigated. Three pairs of synthesized importin β1 or importin α5 siRNAs (see Table S1 in the supplemental material) were transfected into DF-1 cells respectively, and importin β1 RNAi#3 or importin α5 RNAi#2 could effectively lower
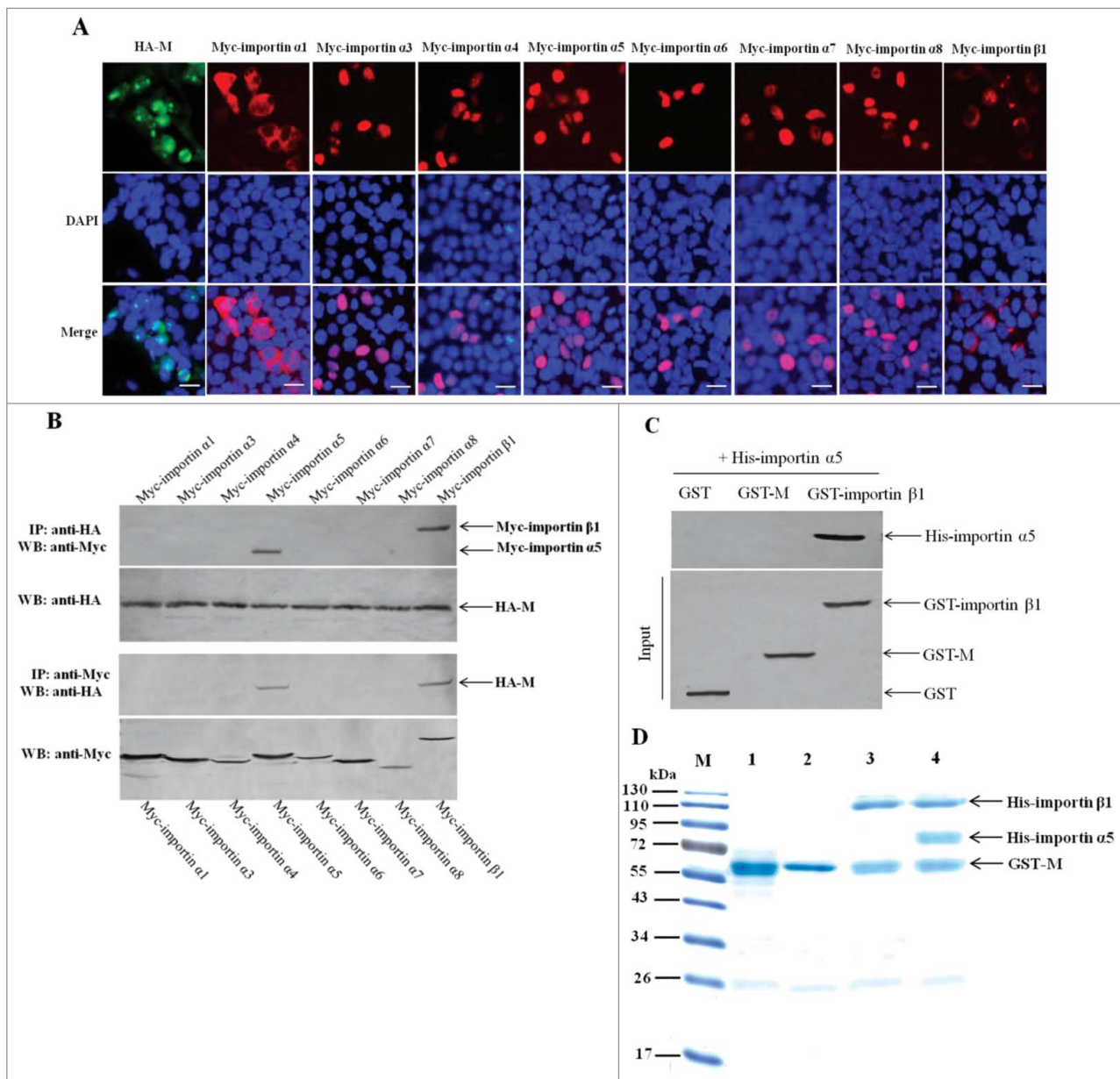
Figure 7. Importin α5 binds NDV M protein by interacting with importin β1. (A) The subcellular localization of the fusion proteins in DF-1 cells. The indicated plasmids were transfected into DF-1 cells and then used for immunofluorescence aasay at 24 h post-transfection. DAPI was used to stain nuclei. Fluorescent images were obtained under a Nikon fluorescence microscope. Original magnification was 1 × 200. (B) Characterization of the interaction between NDV M protein and the cellular transport proteins by reciprocal co-immunoprecipitation assay. DF-1 cells transfected with the plasmids were lysed at 24 h post-transfection, and co-immunoprecipitation assay was performed using either anti-HA (upper panel) or anti-Myc (lower panel) antibodies. Immunoprecipitated proteins were detected by Western blotting using anti-Myc or anti-HA antibodies. (C) Identification of the interaction between importin α5 and M or importin β1 by pull-down assay. The purified GST-M or GST-importin β1 protein was immobilized on Gluthatione-Sepharose beads and then incubated with the purified His-importin α5. The bound proteins were eluted from the beads and examined by Western blotting. (D) Protein binding assay was used to identify the interaction among M, importin α5 and importin β1. Lane 1 was GST-M alone, lane 2 was GST-M plus His-importin α5, lane 3 was GST-M plus His-importin β1, lane 4 was GST-M plus His-importin α5 together with His-importin β1.

the expression level of importin β1 or importin α5 without causing discernable changes in cell morphology (Fig. 8A and B). In addition, the viability of those cells receiving siRNA using trypan blue exclusion and MTT assays were examined. Results showed that there was no difference between importin β1 or importin α5 RNAi and RNAi control in terms of viability of transfected cells (data not shown). We then infected DF-1 cells receiving the indicated siRNA or control siRNA with NDV strain rSS1GFP. As a result, at 6 or 12 hpi, importin β1 depletion caused M protein mainly in the cytoplasm, further confirming that importin β1 mediated the nuclear
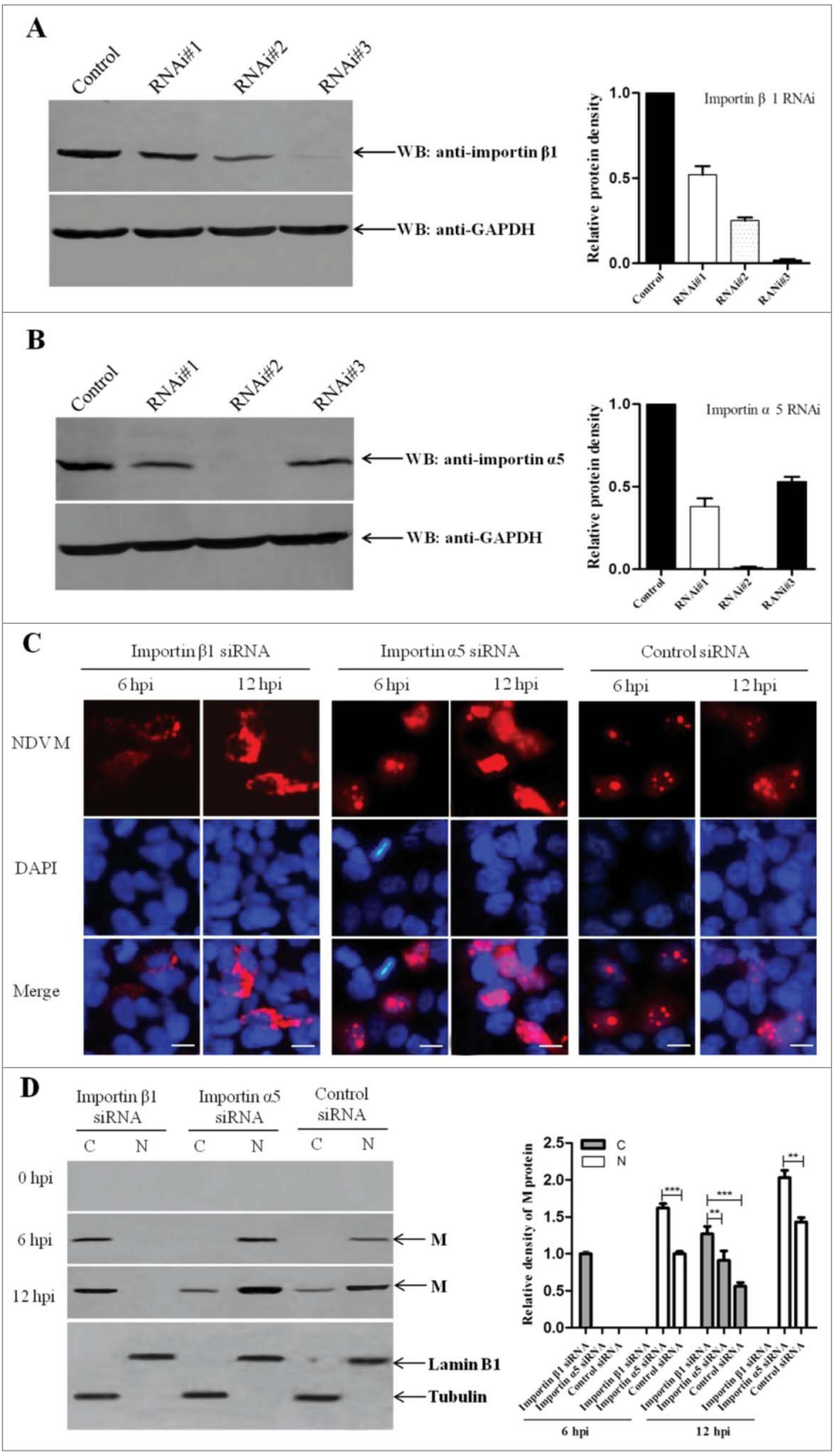
Figure 8. Importin α5 reduces importin β1-mediated nuclear import of NDV M protein. (A and B) Effects of importin β1 or importin α5 RNAi on the expression of endogenous importin β1 or importin α5, respectively. DF-1 cells were transfected with importin β1 or importin α5 siRNA (#1-3) or control siRNA. After 48 h transfection, cell lysates were prepared and examined by Western blot with anti-importin β1 or anti-importin α5 antibody. Endogenous GAPDH expression was used as internal control. (C) DF-1 cells were transfected with importin β1 siRNA or importin α5 siRNA or control siRNA. Forty-eight hours after transfection, cells were infected with rSS1GFP at an MOI of 1. The subcellular localization of NDV M protein in virus-infected DF-1 cells was detected at 6 hpi and 12 hpi, respectively. DAPI was used to stain nuclei. Original magnification was 1 × 200. (D) Immunoblot analysis of the intracellular distribution of M in importin β1 siRNA- or importin α5 siRNA- or control siRNA-treated DF-1 cells. N represents the nucleus and C represents the cytoplasm.

import of M protein. However, importin α5 depletion markedly increased the nuclear accumulation of M protein when compared to that of control siRNA group (Fig. 8C). Similar results were obtained by examining the intracellular distribution of M protein in importin β1 siRNA- or importin α5 siRNA- or control siRNA-treated cells by immunoblot analysis (Fig. 8D). Together with the above results, these data reveal that the importin β1-mediated nuclear import of NDV M protein is reduced in the presence of importin α5.

Importin α5 decreases importin β1-participated NDV replication and pathogenicity

Since importin α5 causes the reduction of nuclear localization of M protein, this might affect the replication and pathogenicity of NDV. To this end, siRNA-mediated knockdown of importin β1 or importin α5 in DF-1 cells infected with NDV strain rSS1GFP was investigated. As shown in Fig. 9A and B, the normal cells and control siRNA-treated cells showed the similar CPE and GFP expression level at 24 hpi, while siRNA-mediated knockdown of importin β1 markedly reduced NDV-induced CPE and GFP expression level, but knockdown of importin α5 greatly enhanced the CPE and GFP expression level when compared to the normal cell group and RNAi control group. In addition, significant reduction of viral loads in the cell culture supernatants and cell pellets of importin β1-RNAi cells was detected, but an increasing of viral loads in that of importin α5-RNAi cells were examined in comparison to that of normal cell and RNAi control (Fig. 9C and D). To further determine the effect of importin β1 or importin α5 knockdown on NDV replication, the mRNA expression levels of NDV M gene in NDV-infected importin β1-RNAi or importin α5-RNAi cells were examined at 24 hpi. We found that the mRNA expression level of NDV M gene in importin β1-RNAi or importin α5-RNAi cells significantly decreased or increased , respectively, in comparison to that of normal cells and RNAi control either in the culture supernatants or in the cell pellets ($P < 0.001$) (Fig. 9E and F). Together, above results demonstrate that importin α5 acts as negative regulator in importin β1-participated NDV replication and pathogenicity in cells.

Discussion

Paramyxoviruses are a diverse group of enveloped viruses with non-segmented negative-sense single-stranded RNA genomes that include a number of important human and animal pathogens [5]. To date, the pathogenic mechanism of the paramyxoviruses still attracts the global researchers' attentions. Two envelope glycoproteins, the attachment protein (termed HN for hemagglutinin-neuraminidase, H for hemagglutinin, or G for glycoprotein, depending on the virus) and the fusion (F) protein, have been always reported to be the major virulence and pathogenic factors for paramyxoviruses [54–56]. However, in recent years, increasing number of researches has focused on the M protein in the pathogenesis of paramyxoviruses due to its multifunction in inhibiting the host RNA and protein synthesis and facilitating the assembly and budding of progeny virions [57–59]. Among the members of paramyxoviruses, the M protein of HRSV, SeV, NiV and NDV is demonstrated to shuttle between the nucleus and cytoplasm through intrinsic NLS and NES [5]. Up to now, only the nucleocytoplasmic shuttling mechanism and the detailed function of HRSV M protein are elucidated [35,36]. We previously have demonstrated that the nuclear export of NDV M protein is mediated by three NESs via the CRM1-independent pathway [60], but the nuclear import mechanism of NDV M protein and the definite functions of M protein in the nucleus are still not known.

Numerous studies have revealed that NLS-mediated nuclear localization of viral proteins is crucial for the replication and pathogenicity of most viruses [28–31]. We previously found that a basic amino acid mutation, R42A, in the NDV M protein not only abrogates its nuclear localization but also attenuates NDV replication and pathogenicity [61]. However, R42A mutation in the M protein does not really reflect the effect of nuclear localization disruption of M protein on the replication and pathogenicity of NDV. Here, we successfully rescued the M/NLS mutant virus rSS1GFP-M/NLSm after three extra chicken egg passages and found that the disruption of M's nuclear localization caused by M/NLS mutation not only resulted in a pathotype change of NDV but also reduced viral replication in cells and attenuated the replication and pathogenicity of NDV in SPF chickens, thus demonstrating for the first time the importance of M's nuclear localization for NDV replication and pathogenicity. In addition, the rescued viruses rSS1GFP and rSS1GFP-M/NLSm could be used to further investigate the more detailed functions of M's nuclear localization in the pathogenesis of NDV utilizing transcriptomics and proteomics. However, it was strange that the MDT and ICPI values of rSS1GFP-M/NLSm did not correlate, which showed that the MDT value suggested the virus was lentogenic, but the ICPI value suggested the virus was velogenic. In our previous studies, we also found that there was no relevance in the MDT and ICPI values of the mutant virus carrying M/F23A (MDT was 102 h, ICPI was 1.64) or M/P24A (MDT was 84 h, ICPI was 1.70) or M/R42A (MDT was 115 h, ICPI was 1.64) when

compared to the parental virus rZJ1GFP (MDT was 52 h, ICPI was 1.91) [61,62]. Another research group has studied the effect of some conserved amino acids mutation in the HN protein on the virulence of NDV. They similarly find that in comparison to the parental virus (MDT is 62 h, ICPI is 1.51), the MDT of Y526Q mutant NDV increases to 98 h, which belongs to the lentogen strain, whereas the ICPI value (1.33) of the virus indicates that
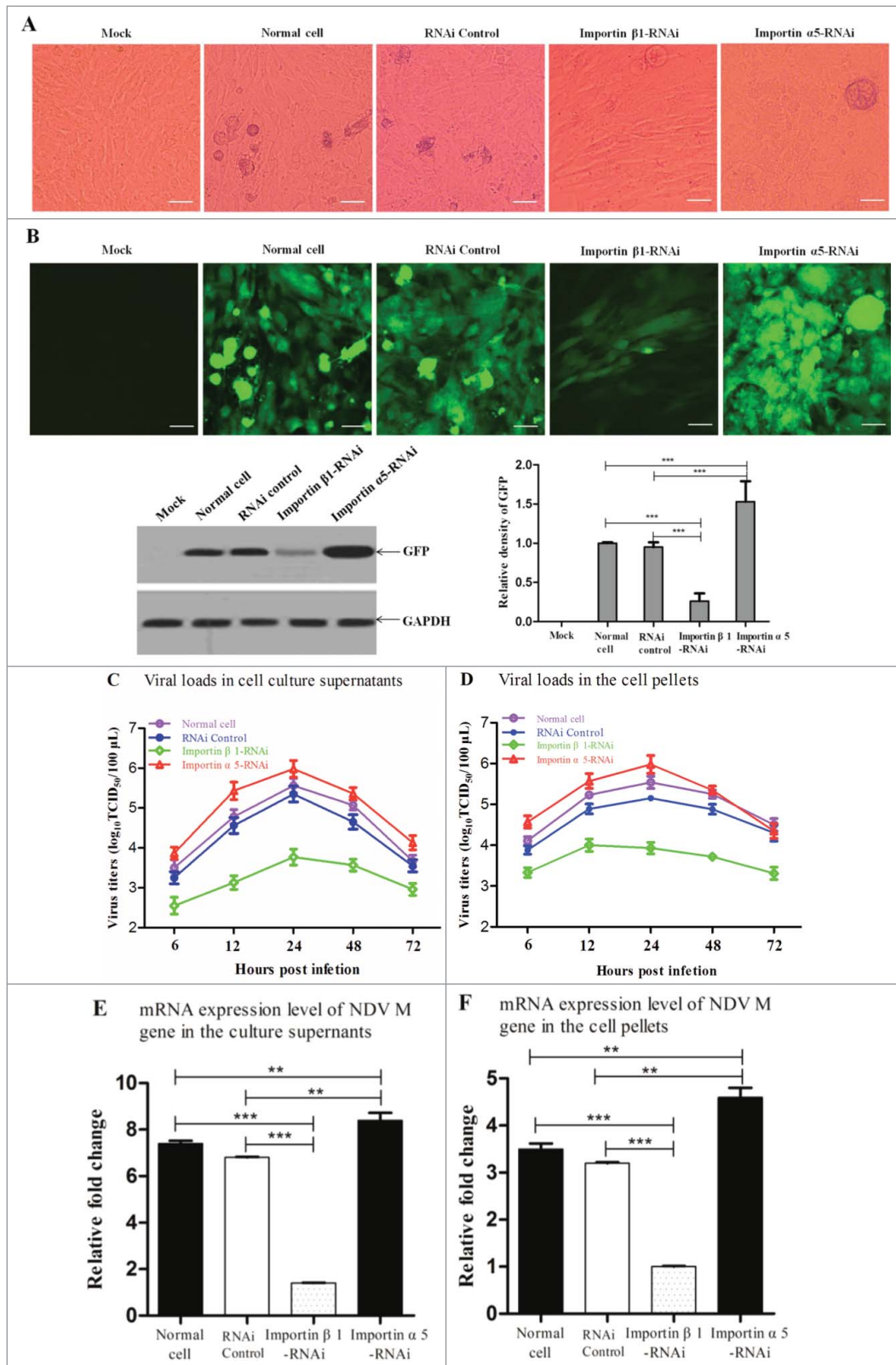

Figure 9. (For figure legend, see page 796.)

10

NDV caused more serious CPE and more increased viral replication ability in comparison to that of normal cells and RNAi control cells. On the contrary, importin β1 depletion not only disrupted the nuclear localization of M protein but also greatly reduced the CPE induced by NDV infection and viral replication capacity. Moreover, we also found that knockdown of importin β1 decreased the expression levels of NDV M protein and GFP in cells. It has been shown that the nuclear localization of paramyxovirus M protein has two main functions: (i) inhibit host gene transcription and protein synthesis, and (ii) ensure that the replication and transcription of viral genome in the cytoplasm proceed until a certain level of viral protein and RNA expression is reached, at which point M is transported into the cytoplasm to participate in virus assembly [57]. Therefore, we speculated that the disruption of M's nuclear localization could not achieve the above functions and led to the reduction of the replication and transcription of viral genome during the course of virus infection. But more experiments were needed to verify the definite nuclear localization functions of NDV M protein. Together with the above results, our studies clearly demonstrated that importin β1 and RanGTP were responsible for the nuclear import process of NDV M protein, and importin β1 alone could increase the nuclear import efficiency of M protein and enhance NDV replication and pathogenicity (Fig. 10A), whereas such case could be decreased in the presence of importin α5 (Fig. 10B).

In summary, we demonstrated for the first time the nuclear import mechanism of NDV M protein and the negative regulation role of importin α5 in importin β1-mediated nuclear import of M protein and the replication and pathogenicity of NDV. Our results will provide a better understanding of the exact role of M's nuclear localization in NDV life cycle and aid in understanding the poorly understood NDV pathogenesis.

Materials and methods

Cells and antibodies

The chicken embryonic fibroblast cell line (DF-1) and HeLa cells were purchased from cell resource center of Shanghai Institutes for Biological Sciences of the Chinese Academy of Sciences. BHK-21 cells (clone BSR-T7/5), generated by Buchholz et al. [76], were a kind gift from Professor Zhigao Bu (Harbin Veterinary Research Institute, China). Primary antibodies goat anti-importin α5 polyclonal antibody (sc-6918), rabbit anti-importin β1 polyclonal antibody (sc-11367), mouse anti-GST monoclonal antibody (sc-374171), mouse anti-His monoclonal antibody (sc-8036), mouse anti-GAPDH monoclonal antibody (sc-66163) were purchased from Santa Cruz

Biotechnology (USA). Mouse anti-GFP monoclonal antibody (ab1218), mouse anti-HA monoclonal antibody (ab18181), rabbit anti-Myc monoclonal antibody (ab32072), rabbit anti-tubulin polyclonal antibody (ab125267) and rabbit anti-Lamin B1 polyclonal antibody (ab16048) were purchased from Abcam (UK).

Plasmids construction

All enzymes used for cloning procedures were purchased from Thermo Scientific Company. The ORF of M gene was amplified from the cDNA derived from the virulent genotype Ⅶd NDV strain Sheldrake duck/China/Guizhou/SS1/2014 (SS1) (GenBank no.KP742770) and then subcloned into pGBKT7, pEGFP-C1, pGEX-6p-1, pCMV-HA, pGEX-GFP to generate pGBKT7-M, pEGFP-M, pGEX-6p-M, pCMV-HA-M and pGEX-M-GFP, respectively. The chicken importin β1 or importin α5 ORF was amplified from the cDNA derived from DF-1 cells and then used to construct the plasmids pET-32a-importin β1, pCMV-Myc-importin β1, pGEX-6p-importin β1 and pET-32a-importin α5, respectively. Annealed oligonucleotides encoding the M9M [45] or Bimax2 [46] were inserted into pDsRed-C1 (Clontech) to generate plasmids pDsRed-M9M and pDsRed-Bimax2, respectively. Dominant negative (DN) mutant DN importin α5, DN mutant NTF2 (NTF2/E42K), DN importin β1 or RanQ69L was subcloned into pDsRed-C1 to yield pDsRed-DN-importin α5, pDsRed-DN-NTF2/E42K, pDsRed-DN-importin β1 and pDsRed-RanQ69L, respectively.

To generate the recombinant infectious clones harboring alanine (A) substitution targeting basic amino acid residues in the NLS motif (^{247}AAGAAVIFDKIEEKIAA^{263}) of M protein, the fragment containing the restriction enzyme sties Age Ⅰ and BstZ17 Ⅰ was amplified by two pairs of specific primers, which were used to introduce multiple amino acid substitutions in the M protein, to generate two overlapping PCR fragments. The two PCR fragments were joined in a second PCR and the obtained fragment was digested with Age Ⅰ and BstZ17 Ⅰ to replace the corresponding region in the full-length cDNA clone pNDV/SS1GFP (see Figure S2 in the supplemental material) [77]. The resulting plasmid was named pNDV/SS1GFP-M/NLSm. All the recombinant plasmids were confirmed by PCR, restriction digestion and DNA sequencing. Primers used in this study are available upon request.

Yeast two-hybrid screening and colony-lift filter assay

The yeast AH109 containing bait plasmid pGBKT7-M was grown on SD/-Trp/X-α-gal, SD/-Trp/-His/X-α-gal and SD/-Trp/-Ade/X-α-gal to exclude the autonomous
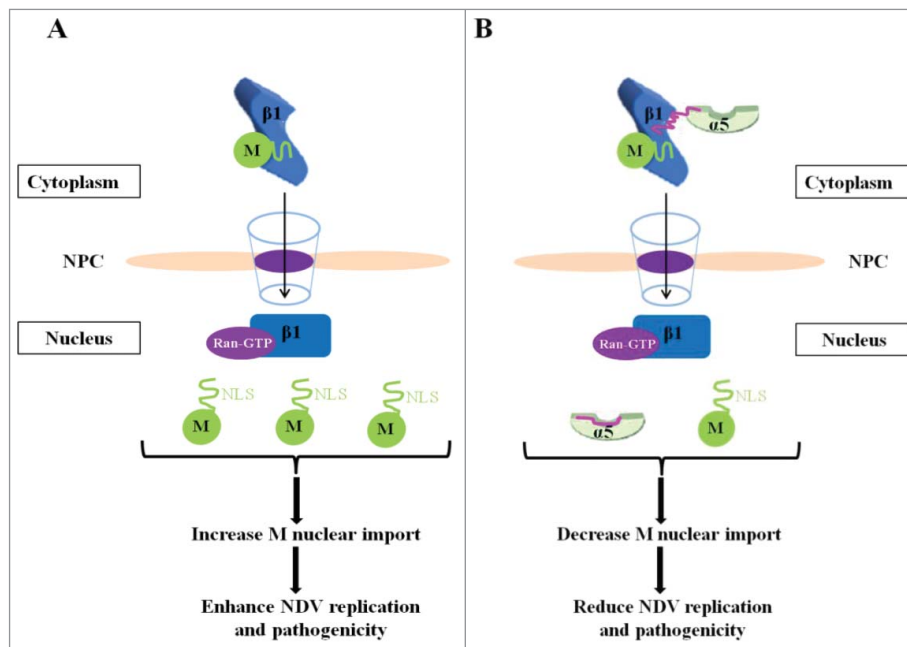
Figure 10. The schematic diagram of the negative regulation role of importin α5 in importin β1-mediated nuclear import of M protein and the replication and pathogenicity of NDV.

transcriptional activity. Then the transformed AH109 mated with yeast Y187 containing pGADT7-Rec with the cDNA library of DF-1 cells for 24 h. The screening was performed according to the manufacturer's instructions (Matchmaker^{TM} GAL4 Two-Hybrid System 3) and as previously described [78]. In β-galactosidase colony-filter assay, the prey plasmids in the suspected positive clones were rescued and then co-transformed into AH109 with the plasmid pGBKT7-M. Positive clones grown on SD/-Ade/-His/-Trp/-Leu medium were tested for β-galactosidase activity. The pGBKT7-53 and pGADT7-T or pGBKT7-Lam and pGADT7-T co-transformed group was used as a positive and negative control, respectively. Yeast colonies co-transformed with pGBKT7-M and the pGADT7-derivative plasmids were checked periodically for the appearance of blue colonies. Yeast plasmid was isolated from blue colonies as previously described [79], and the inserted fragment was obtained by PCR amplification and then analyzed by bioinformatics methods.

Cell culture, transfection and fluorescence microscopy

DF-1 cells were cultured in Dulbecco's modified Eagle's medium (DMEM, GIBCO) containing 10% fetal bovine serum (FBS, GIBCO) supplemented with 100 U/ml penicillin and 100 μg/ml streptomycin at 37°C under an atmosphere with 5% CO_2. For the transfection experiments, 4×10^5 DF-1 cells were grown to 80% confluence in 35-mm-diameter dishes and then double or single transfected with a total of 3 μg plasmid using the FuGENE HD Transfection Reagent (Roche) according to the manufacturer's recommendations. Twenty-four hours after transfection, cells expressing the fluorescence-fused proteins were rinsed with phosphate-buffered saline (PBS), fixed with 4% paraformaldehyde for 20 min, permeabilized with 0.25% Triton X-100 in PBS for 5 min, and then counterstained with DAPI (Sigma) to detect the nuclei. Fluorescent images were obtained under a Nikon fluorescence microscope (Japan). Analysis and merging of the images were done with Adobe Photoshop 7.0 software.

Protein interaction assays

For co-immunoprecipitation assay, 4×10^5 DF-1 cells grown in 35-mm-diameter dishes were transfected with plasmid pCMV-Myc-importin β1 for 24 h and then infected with NDV strain rSS1GFP at a multiplicity of infection (MOI) of 0.1. On the other hand, DF-1 cells cultured in 35 mm dishes were co-transfected with pCMV-HA-M and the indicated plasmids. At 24 h post-infection or post-transfection, cells were washed and lysed with immunoprecipitation buffer. After centrifugation, the supernatants were collected and incubated with the corresponding antibodies overnight at 4°C. The immune complexes were recovered by adsorption to protein A+G-Sepharose (Sigma) for 3 h at 4°C. After three washes in immunoprecipitation buffer, the immunoprecipitates were detected by Western blotting.

For pull-down assays, the His-importin β1 or His-importin β1($\triangle$336–433) or His-importin α5 fusion

protein was expressed in *E. coli* BL21 (DE3) (4 h induction with 1.0 mM IPTG at 30°C), and the soluble His-tagged proteins were purified on Ni-NTA His Bind Resin. GST-M and GST-M/NLSm (4 h induction with 0.5 mM IPTG at 28°C), and GST-importin β1 (4 h induction with 1.0 mM IPTG at 30°C) were expressed in *E. coli* BL21 (DE3), respectively, and the soluble fusion proteins were purified on Glutathione-Sepharose beads. In the GST pull-down experiments, the purified GST-M or GST-M/NLSm or GST-importin β1 protein was immobilized on Gluthatione-Sepharose beads (3 μg protein/10 μL beads). After washing with transport buffer, the immobilized proteins were incubated with the purified His-importin β1 or His-importin β1($\triangle$336–433) or His-importin α5 (3 μg for each protein, total volume 40 μL) for 2 h at 4°C. The beads were then washed three times with transport buffer and the bound proteins were eluted from the beads and used for SDS-PAGE followed by Coomassie blue staining or Western blot analysis. In the His pull-down experiments, His*Bind Resin-binded His-importin β1 or His-importin β1 ($\triangle$336-433) (3 μg protein/10 μL resins) was incubated with purified GST-M (3 μg) for 2 h at 4°C. The resins were dealt with as described above, and the target protein GST-M was detected by Western blotting.

In vitro nuclear import assays

In vitro nuclear import assays in digitonin-permeabilized cells were performed as previously described [80]. Briefly, subconfluent HeLa cells were cultured on poly-L-lysine-coated glass coverslips for 1 day and then permeabilized with 70 μg of digitonin/ml for 5 min on ice. The digitonin-permeabilized HeLa cells were rinsed twice with transport buffer and then incubated for 15 min at room temperature with the import mixture. Import reactions contained an energy regenerating system (0.5 mM GTP, 5 mM phosphocreatine, and 0.4 U of creatine phosphokinase), plus various transport factors (0.5 μM importin β1; 3 μM RanGTP; 3 μM RanGDP; 3 μM RanQ69LGTP), plus the GST-M-GFP fusion protein (0.5 μM). The final reaction volume was adjusted to 20 μL with transport buffer. After incubation, the cells were washed with transport buffer and fixed with 3.7% formaldehyde on ice followed by methanol for 5 min at -20°C. After three washes with transport buffer, the nuclei were identified by DAPI staining. The results of GST-M-GFP nuclear import were analyzed with a Nikon fluorescence microscope.

Virus rescue and pathogenicity assay

For the virus rescue, BSR-T7/5 cells were grown in DMEM medium containing 10% FBS and 1 mg/ml geneticin G418 for five generation before transfection. Cells at 70% confluence in 35 mm dishes were transfected with the full-length cDNA clone (pNDV/SS1GFP or pNDV/SS1GFP-M/NLSm) together with three SS1-derived helper plasmids at a total of 3 μg [77]. At 60 h post-transfection, the cell monolayers and culture supernatants were harvested and inoculated into the allantoic cavities of 10-day-old embryonated SPF chicken eggs. The HA test and DNA sequencing were performed to identify the rescued viruses rSS1GFP and rSS1GFP-M/NLSm. Plaque formation assays and viral titers were performed using standard methods [81]. The pathogenicity assay of the rescued viruses was determined using the standard pathogenicity tests: the MDT test in 10-day-old SPF chicken eggs, and the ICPI test in 1-day-old SPF chicks [81].

Pathogenicity assessment of the rescued viruses in 4-week-old chickens

The pathogenicity assessment of the rescued viruses rSS1GFP and rSS1GFP-M/NLSm was determined in 4-week-old SPF chickens. Forty-eight chickens were assigned randomly into three experimental groups, consisting of rSS1GFP- (n = 16), rSS1GFP-M/NLSm- (n = 16) and mock- (PBS, n = 16) infected groups. For each group, 6 birds and 10 birds were used for sampling and clinical observation, respectively. Chickens were inoculated via the eye drop/intranasal route with each virus at a dose of $10^{5.0}$ EID$_{50}$/100 μL per bird, or with 100 μL PBS as the negative control. The birds were monitored for clinical signs daily for 10 dpi. Three birds were euthanized daily from 4–5 dpi for gross lesion observation, and samples of the heart, liver, spleen, lung, kidney, brain, trachea, duodenum, bursa of Fabricius and thymus were collected to detect virus titration in DF-1 cells at 5 dpi. The virus titers were determined as the TCID$_{50}$ per gram (log$_{10}$TCID$_{50}$ g^{-1} tissue) using the endpoint method of Reed and Muench. The part of collected lymphoid tissues (spleen, thymus and bursa of Fabricius) was fixed in 10% neutral formalin, routinely sectioned and stained with hematoxylin-eosin, and then examined for lesions using Nikon light microscopy.

Immunofluorescence antibody assay

DF-1 cells grown in 12-well plates were treated with the drug ivermectin or DMSO as described previously [82]. Cells were then infected with NDV strain rSS1GFP at an MOI of 0.1 and prepared for immunofluorescence analysis at 12 hpi. At the stipulated time, cells were rinsed with PBS, fixed with 4% paraformaldehyde for 20 min, and then permeabilized with 0.2% Triton X-100 in PBS

for 5 min. Cells were rinsed with PBS and blocked with 10% FBS in PBS for 30 min, and then incubated with anti-M polyclonal antibodies diluted in PBS containing 10% FBS for 1 h [16]. After three washes with PBS, the cells were incubated with Alexa Fluor 488 goat anti-rabbit immunoglobulin G antibody (Invitrogen) for 1 h. Cells were counterstained with DAPI to detect nuclei. For siRNA experiments, siRNA-transfected DF-1 cells were infected with rSS1GFP at an MOI of 1, and cells were collected at 6 hpi or 12 hpi to perform immunofluorescence antibody assay as described above. Images were captured with a fluorescence microscope and processed with Adobe Photoshop 7.0 software.

siRNA treatment and virus infection

The sequences of three pairs of siRNA designed to knockdown importin $\beta1$ or importin $\alpha5$ in DF-1 cells were shown in supplemental Table S1. Negative siRNA control (Cat. No.12935-400) and siRNA transfection reagent were purchased from Invitrogen. For transfection with the siRNA against importin $\beta1$ or importin $\alpha5$, low-passage DF-1 cells were transfected with the indicated siRNAs at a confluence of 80% on 35 mm dishes, and the knockdown efficiency was checked by immunoblot analysis at 48 h post-transfection. To study the effect of importin $\beta1$ or importin $\alpha5$ knockdown on the subcellular localization of M protein and the replication of NDV, the NDV strain rSS1GFP was used to infect importin $\beta1$ or importin $\alpha5$ siRNA-treated DF-1 cells at an MOI of 1. The subcellular localization of M protein was examined by immunofluorescence assay and immunoblotting analysis and at 6 hpi and 12 hpi, respectively. In addition, the cell culture supernatants and cell pellets were collected at the indicated time points (6, 12, 24, 48, and 72 hpi), and the virus titers were determined as 50% tissue culture infective dose ($TCID_{50}$) in DF-1 cells [78]. Moreover, the CPE and green fluorescence in virus-infected cells were observed under fluorescence microscope and the GFP expression level was detected by Western blotting at 24 hpi.

RNA isolation and qRT-PCR analysis

Total RNA was prepared from siRNA-treated DF-1 cells using Qiagen RNeasy kit according to the manufacturer's protocol. One microgram of total RNA was used for cDNA synthesis by reverse transcription kit (TaKaRa). For quantification of the mRNA of NDV M gene, a SYBR green-based real-time PCR method (TaKaRa) was used, and GAPDH mRNA was quantified to normalize the total RNA concentration between different samples. The primers for detecting the M gene

and GAPDH gene were designed with reference to previous publication [16]. The real-time PCR operation was carried out according to the previously described method [78]. The standard cure method was used to analyze the fold change of M gene mRNA expression level. For cell pellets analysis, the NDV M gene expression levels were calculated relatively to the expression of the GAPDH gene. The relative fold change of M gene expression in the cell pellets was calculated as follows: (mRNA expressions of M gene/GAPDH in Control RNAi or Normal cells)/ (mRNA expressions of M gene/GAPDH in importin $\beta1$ or importin $\alpha5$ RNAi cells). The relative fold change of M gene expression in the cell supernatants was calculated as follows: (mRNA expressions of M gene in Control RNAi or Normal cell culture)/ (mRNA expressions of M gene in importin $\beta1$ or importin $\alpha5$ RNAi cell culture).

Statistical analysis

Statistical analysis was performed using the GraphPad Prism 6.0 software (GraphPad Software Inc., La Jolla, CA, USA). The p-values between identified samples were generated using unpaired two-tailed Student's t-test. All experiments were repeated at least three times and the results were presented as the mean $\pm$ standard deviation (SD). The significance levels were defined as $P < 0.05$.

Abbreviations

NDV	Newcastle disease virus
HRSV	human respiratory syncytial virus
VSV	vesicular stomatitis virus
MeV	measles virus
SeV	Sendai virus
NiV	Nipah virus
SPF	specific pathogen free
hpi	hours post-infection
dpi	days post-infection
CPE	cytopathic effect
EID_{50}	50% egg infectious dose
$TCID_{50}$	50% tissue culture infective dose
NLS	nuclear localization signal
NoLS	nucleolar localization signal
NES	nuclear export signal
NPC	nuclear pore complex
RanGDP	GDP-bound small GTPase Ran
RanGTP	GTP-bound small GTPase Ran

Disclosure of potential conflicts of interest

No potential conflicts of interest were disclosed.

Acknowledgments

Funding

References

[1] Miller PJ, Decanini EL, Afonso CL. Newcastle disease: evolution of genotypes and the related diagnostic challenges. Infect Genet Evol. 2010;10:26–35.

[2] Ganar K, Das M, Sinha S, et al. Newcastle disease virus: current status and our understanding. Virus Res. 2014;184:71–81.

[3] Duan ZQ, Xu HQ, Ji XQ, et al. Recombinant Newcastle disease virus-vectored vaccines against human and animal infectious diseases. Future Microbiol. 2015;10:1307–23.

[4] Battisti AJ, Meng G, Winkler DC, et al. Structure and assembly of a paramyxovirus matrix protein. Proc Natl Acad Sci U S A. 2012;109:13996–4000.

[5] Harrison MS, Sakaguchi T, Schmitt AP. Paramyxovirus assembly and budding: building particles that transmit infections. Int J Biochem Cell Biol. 2010;42:1416–29.

[6] Pantua HD, McGinnes LW, Peeples ME, et al. Requirements for the assembly and release of Newcastle disease virus-like particles. J Virol. 2006;80:11062–73.

[7] Peeples ME. Differential detergent treatment allows immunofluorescent localization of the Newcastle disease virus matrix protein within the nucleus of infected cells. Virology. 1988;162:255–9.

[8] Peeples ME, Wang C, Gupta KC, et al. Nuclear entry and nucleolar localization of the Newcastle disease virus (NDV) matrix protein occur early in infection and do not require other NDV proteins. J Virol. 1992;66:3263–9.

[9] Duan Z, Li QH, He L, et al. Application of green fluorescent protein-labeled assay for the study of subcellular localization of Newcastle disease virus matrix protein. J Virol Methods. 2013;194:118–22.

[10] Ghildyal R, Baulch-Brown C, Mills J, et al. The matrix protein of human respiratory syncytial virus localises to the nucleus of infected cells and inhibits transcription. Arch Virol. 2003;148:1419–29.

[11] Rajani KR, Pettit Kneller EL, McKenzie MO, et al. Complexes of vesicular stomatitis virus matrix protein with host Rae1 and Nup98 involved in inhibition of host transcription. PLoS Pathog. 2012;8:e1002929.

[12] Iwasaki M, Takeda M, Shirogane Y, et al. The matrix protein of measles virus regulates viral RNA synthesis and assembly by interacting with the nucleocapsid protein. J Virol. 2009;83:10374–83.

[13] Hiscox JA, Whitehouse A, Matthews DA. Nucleolar proteomics and viral infection. Proteomics. 2010;10:4077–86.

[14] Rawlinson SM, Moseley GW. The nucleolar interface of RNA viruses. Cell Microbiol. 2015;17:1108–20.

[15] Wulan WN, Heydet D, Walker EJ, et al. Nucleocytoplasmic transport of nucleocapsid proteins of enveloped RNA viruses. Front Microbiol. 2015;6:553.

[16] Duan Z, Chen J, Xu H, et al. The nucleolar phosphoprotein B23 targets Newcastle disease virus matrix protein to the nucleoli and facilitates viral replication. Virology. 2014;452–453:212–22.

[17] Coleman NA, Peeples ME. The matrix protein of Newcastle disease virus localizes to the nucleus via a bipartite nuclear localization signal. Virology. 1993;195:596–607.

[18] Pouton CW, Wagstaff KM, Roth DM, et al. Targeted delivery to the nucleus. Adv Drug Deliv Rev. 2007;59:698–717.

[19] Twyffels L, Gueydan C, Kruys V. Transportin-1 and Transportin-2: protein nuclear import and beyond. FEBS Lett. 2014;588:1857–68.

[20] Miyamoto Y, Yamada K, Yoneda Y. Importin α: a key molecule in nuclear transport and non-transport functions. J Biochem. 2016;160:69–75.

[21] Goldfarb DS, Corbett AH, Mason DA, et al. Importin α: a multipurpose nuclear-transport receptor. Trends Cell Biol. 2004;14:505–14.

[22] Lange A, Mills RE, Lange CJ, et al. Classical nuclear localization signals: definition, function, and interaction with importin alpha. J Biol Chem. 2007;282:5101–5.

[23] Xu DR, Farmer A, Chook YM. Recognition of nuclear targeting signals by karyopherin-β proteins. Curr Opin Struc Biol. 2010;20:782–90.

[24] Lott K, Cingolani G. The importin beta binding domain as a master regulator of nucleocytoplasmic transport. Biochim Biophys Acta. 2011;1813:1578–92.

[25] Soniat M, Chook YM. Nuclear localization signals for four distinct karyopherin-beta nuclear import systems. Biochem J. 2015;468:353–62.

[26] Sekimoto T, Miyamoto Y, Arai S, et al. Importin alpha protein acts as a negative regulator for Snail protein nuclear import. J Biol Chem. 2011;286:15126–31.

[27] Forwood JK, Jans DA. Nuclear import pathway of the telomere elongation suppressor TRF1: inhibition by importin alpha. Biochemistry. 2002;41:9333–40.

[28] Lopez-Denman AJ, Mackenzie JM. The importance of the nucleus during flavivirus replication. Viruses. 2017;9:e14.

[29] Tu MY, Liu F, Chen S, et al. Role of capsid proteins in parvoviruses infection. Virol J. 2015;12:114.

[30] Wang C, Zhu CX, Wei F, et al. Nuclear localization and cleavage of STAT6 is induced by Kaposi's sarcoma-associated herpesvirus for viral latency. PLoS Pathog. 2017;13:e1006124.

[31] Widana Gamage SMK, Dietzgen RG. Intracellular localization, interactions and functions of Capsicum chlorosis virus proteins. Front Microbiol. 2017;8:612.

[32] Lee C, Hodgins D, Calvert JG, et al. Mutations within the nuclear localization signal of the porcine reproductive

and respiratory syndrome virus nucleocapsid protein attenuate virus replication. Virology. 2006;346:238–50.

[33] Mori Y, Okabayashi T, Yamashita T, et al. Nuclear localization of Japanese encephalitis virus core protein enhances viral replication. J Virol. 2005;79:3448–58.

[34] Katoh H, Okamoto T, Fukuhara T, et al. Japanese encephalitis virus core protein inhibits stress granule formation through an interaction with caprin-1 and facilitates viral propagation. J Virol. 2013;87:489–502.

[35] Ghildyal R, Ho A, Wagstaff KM, et al. Nuclear import of the respiratory syncytial virus matrix protein is mediated by importin beta1 independent of importin alpha. Biochemistry. 2005;44:12887–95.

[36] Ghildyal R, Ho A, Dias M, et al. The respiratory syncytial virus matrix protein possesses a Crm1-mediated nuclear export mechanism. J Virol. 2009;83:5353–62.

[37] Quan Y, Ji ZL, Wang X, et al. Evolutionary and transcriptional analysis of karyopherin beta superfamily proteins. Mol Cell Proteomics. 2008;7:1254–69.

[38] Huang Y, Zhang J, Halawa MA, et al. Nuclear localization signals of varicella zoster virus ORF4. Virus Genes. 2014;48:243–51.

[39] Li Y, Zhao L, Wang SA, et al. Identification of a novel NLS of herpes simplex virus type 1 (HSV-1) VP19C and its nuclear localization is required for efficient production of HSV-1. J Gen Virol. 2012;93:1869–75.

[40] Li ML, Wang SA, Cai MS, et al. Characterization of molecular determinants for nucleocytoplasmic shuttling of PRV UL54. Virology. 2011;417:385–93.

[41] Cheng F, McLaughlin PJ, Zagon IS. Regulation of cell proliferation by the opioid growth factor receptor is dependent on karyopherin beta and Ran for nucleocytoplasmic trafficking. Exp Biol Med. 2010;235:1093–101.

[42] Kurisaki A, Kose S, Yoneda Y, et al. Transforming growth factor-beta induces nuclear import of Smad3 in an importin-beta1 and Ran-dependent manner. Mol Biol Cell. 2001;12:1079–91.

[43] Reid SP, Valmas C, Martinez O, et al. Ebola virus VP24 proteins inhibit the interaction of NPI-1 subfamily karyopherin alpha proteins with activated STAT1. J Virol. 2007;81:13469–77.

[44] Guo H, Mao R, Block TM, et al. Production and function of the cytoplasmic deproteinized relaxed circular DNA of hepadnaviruses. J Virol. 2010;84:387–96.

[45] Cansizoglu AE, Lee BJ, Zhang ZC, et al. Structure-based design of a pathway-specific nuclear import inhibitor. Nat Struct Mol Biol. 2007;14:452–4.

[46] Kosugi S, Hasebe M, Entani T, et al. Design of peptide inhibitors for the importin alpha/beta nuclear import pathway by activity-based profiling. Chem Biol. 2008;15:940–9.

[47] Palacios I, Weis K, Klebe C, et al. RAN/TC4 mutants identify a common requirement for snRNP and protein import into the nucleus. J Cell Biol. 1996;133:485–94.

[48] Clarkson WD, Corbett AH, Paschal BM, et al. Nuclear protein import is decreased by engineered mutants of nuclear transport factor 2 (NTF2) that do not bind GDP-Ran. J Mol Biol. 1997;272:716–30.

[49] Ribbeck K, Lipowsky G, Kent HM, et al. NTF2 mediates nuclear import of Ran. EMBO J. 1998;17:6587–98.

[50] Wagstaff KM, Sivakumaran H, Heaton SM, et al. Ivermectin is a specific inhibitor of importin α/β-mediated nuclear import able to inhibit replication of HIV-1 and dengue virus. Biochem J. 2012;443:851–6.

[51] Köhler M, Fiebeler A, Hartwig M, et al. Differential expression of classical nuclear transport factors during cellular proliferation and differentiation. Cell Physiol Biochem. 2002;12:335–44.

[52] Pumroy RA, Cingolani G. Diversification of importin-alpha isoforms in cellular trafficking and disease states. Biochem J. 2015;466:13–28.

[53] Kimoto C, Moriyama T, Tsujii A, et al. Functional characterization of importin $\alpha 8$ as a classical nuclear localization signal receptor. Biochim Biophys Acta. 2015;1853:2676–83.

[54] Smith EC, Popa A, Chang A, et al. Viral entry mechanisms: the increasing diversity of paramyxovirus entry. FEBS J. 2009;276:7217–27.

[55] Plattet P, Plemper RK. Envelope protein dynamics in paramyxovirus entry. MBio. 2013;4:e00413–13.

[56] Dortmans JC, Koch G, Rottier PJ, et al. Virulence of Newcastle disease virus: what is known so far? Vet Res. 2011;42:122.

[57] Ghildyal R, Ho A, Jans DA. Central role of the respiratory syncytial virus matrix protein in infection. FEMS Microbiol Rev. 2006;30:692–705.

[58] Wang YE, Park A, Lake M, et al. Ubiquitin-regulated nuclear-cytoplasmic trafficking of the Nipah virus matrix protein is important for viral budding. PLoS Pathogen. 2010;6:e1001186.

[59] Watkinson RE, Lee B. Nipah virus matrix protein: expert hacker of cellular machines. FEBS Lett. 2016;590:2494–511.

[60] Duan Z, Song Q, Wang Y, et al. Characterization of signal sequences determining the nuclear export of Newcastle disease virus matrix protein. Arch Virol. 2013;158:2589–95.

[61] Duan Z, Li J, Zhu J, et al. A single amino acid mutation, R42A, in the Newcastle disease virus matrix protein abrogates its nuclear localization and attenuates viral replication and pathogenicity. J Gen Virol. 2014;95:1067–73.

[62] Duan Z, Hu Z, Zhu J, et al. Mutations in the FPIV motif of Newcastle disease virus matrix protein attenuate virus replication and reduce virus budding. Arch Virol. 2014;159:1813–9.

[63] Khattar SK, Yan Y, Panda A, et al. A Y526Q mutation in the Newcastle disease virus HN protein reduces its functional activities and attenuates virus replication and pathogenicity. J Virol. 2009;83:7779–82.

[64] Palmeri D, Malim MH. Importin beta can mediate the nuclear import of an arginine-rich nuclear localization signal in the absence of importin alpha. Mol Cell Biol. 1999;19:1218–25.

[65] Truant R, Cullen BR. The arginine-rich domains present in human immunodeficiency virus type 1 Tat and Rev function as direct importin beta-dependent nuclear localization signals. Mol Cell Biol. 1999;19:1210–7.

[66] Xiao Z, Liu X, Lodish HF. Importin beta mediates nuclear translocation of Smad 3. J Biol Chem. 2000;275:23425–8.

[67] Bai L, Michael WM, Yan S. Importin β-dependent nuclear import of TopBP1 in ATR-Chk1 checkpoint in Xenopus egg extracts. Cell Signal. 2014;26:857–67.

[68] Duan ZQ, Zhao JF, Xu HQ, et al. Characterization of the nuclear import pathway for BLM protein. Arch Biochem Biophys. 2017;634:57–68.

[69] Nadler SG, Tritschler D, Haffar OK, et al. Differential expression and sequence-specific interaction of karyopherin alpha with nuclear localization sequences. J Biol Chem. 1997;272:4310–5.

[70] Tsuji L, Takumi T, Imamoto N, et al. Identification of novel homologues of mouse importin alpha, the alpha subunit of the nuclear pore-targeting complex, and their tissue-specific expression. FEBS Lett. 1997;416:30–4.

[71] Zachariae U, Grubmuller H. Importin-beta: structural and dynamic determinants of a molecular spring. Structure. 2008;16:906–15.

[72] Conti E, Muller CW, Stewart M. Karyopherin flexibility in nucleocytoplasmic transport. Curr Opin Struct Biol. 2006;16:237–44.

[73] Cingolani G, Bednenko J, Gillespie MT, et al. Molecular basis for the recognition of a nonclassical nuclear localization signal by importin beta. Mol Cell. 2002;10:1345–53.

[74] Choi S, Yamashita E, Yasuhara N, et al. Structural basis for the selective nuclear import of the C2H2 zinc-finger protein Snail by importin β. Acta Crystallogr D Biol Crystallogr. 2014;70:1050–60.

[75] Lee SJ, Sekimoto T, Yamashita E, et al. The structure of importin-beta bound to SREBP-2: nuclear import of a transcription factor. Science. 2003;302:1571–5.

[76] Buchholz UJ, Finke S, Conzelmann KK. Generation of bovine respiratory syncytial virus (BRSV) from cDNA: BRSV NS2 is not essential for virus replication in tissue culture, and the human RSV leader region acts as a functional BRSV genome promoter. J Virol. 1999;73:251–9.

[77] Duan ZQ, Ji XQ, Xu HQ, et al. Rescue of duck-origin virulent Newcastle disease virus from cloned cDNA and stable expression of the red fluorescent protein. Virol Reports.2016:97–103.

[78] Li X, Li X, Cao H, et al. Engagement of new castle disease virus (NDV) matrix (M) protein with charged multivesicular body protein (CHMP) 4 facilitates viral replication. Virus Res. 2013;171:80–8.

[79] Wang MQ, Wang LL, Guo Y, et al. The broad pattern recognition spectrum of the Toll-like receptor in mollusk Zhikong scallop Chlamys farreri. Dev Comp Immunol. 2015;52:192–201.

[80] Merle E, Rose RC, LeRoux L, et al. Nuclear import of HPV11 L1 capsid protein is mediated by karyopherin $\alpha2\beta1$ heterodimers. J Cell Biochem. 1999;74:628–37.

[81] Alexander DJ. In A Laboratory Manual for the Isolation and Identification of Avian Pathogens, 3rd edn, pp.114–120. Edited by H. G. Purchase, L. H. Arp, C. H. Domermuth, & J. E. Pearson. Kennett Square, PA: American Association for Avian Pathologists, Inc. 1989;

[82] Lundberg L, Pinkham C, Baer A, et al. Nuclear import and export inhibitors alter capsid protein distribution in mammalian cells and reduce Venezuelan Equine Encephalitis Virus replication. Antiviral Res. 2013;100:662–72.